JOURNAL OF MATERIALS SCIENCE 14 (1979) 1187–1191

Deformation parameters in single steel wire–copper matrix composites

SHOJIRO OCHIAI, YOTARO MURAKAMI
Department of Metallurgy, Faculty of Engineering, Kyoto University, Kyoto 606, Japan

By using the single carbon-steel fibre–copper matrix composites, the important parameters controlling dislocation motions in the fibre, matrix and composite, namely flow stress, internal stress, effective stress, change in flow stress due to change in strain-rate or temperature, stress exponent of strain-rate, effective stress exponent of dislocation velocity, activation volume and activation enthalpy were measured at the stage in which the mechanical interaction between the components was negligible. It was found that all the composite parameters were determined only by the properties of the components and for each parameter, a modified rule of mixtures was derived.

1. Introduction

On a macro-scale, much of the deformation behaviour of fibre-composite materials has been shown to obey the rule of mixtures (ROM) [1, 2], i.e. a property of a composite as a whole is determined by the volume-fraction weighted sum of that property for fibre and matrix. However, macro-scale study deals only with the apparent macroscopic properties and fails to clarify the essence of deformation, since the deformation behaviour of composites is essentially connected to dislocation motions in composites. Not only in the light of macro-scale study but also in the light of dislocation motions, the deformation behaviour of composites should be investigated.

Recently, the dynamic nature of plastic deformation of metals and its relation to thermally activated dislocation mechanisms have been widely investigated. However, for composites, they have not yet been studied. The aims of this paper are to measure the various important parameters concerned with dislocation motions in fibre, matrix and composite, and then to derive a modified ROM for each parameter using the deformation stage III-(1) [3] where the constraint effects due to the difference in Poisson's ratios between the components [4], and those due to suppression of necking in the fibre [5], do not exist. In this work, a modified ROM for the following parameters will be derived; (1) flow stress, internal stress and effective stress, (2) changes in flow stress due to change in strain-rate and temperature, (3) stress exponent of strain-rate and effective stress exponent of dislocation velocity, (4) activation volume, and (5) activation enthalpy.

In the present work, 0.1% carbon-steel and copper were employed as fibre and matrix materials, respectively, because of the large differences in their parameters [6, 7]. The specimens used in this study were thick single fibre-composites so that small-fibre strengthening of the matrix [8, 9] could be precluded and also the effects of neighbouring fibres [5, 10] eliminated.

2. Experimental procedure

The fibres and matrix employed were 0.1% carbon-steel wire of 500 μm and pure copper, respectively. First the fibres were cleaned with acetone and etchant (5% HNO_3 + 95% C_2H_5OH) to remove surface lubricant and oxides, and then they were rinsed in water. The composite specimens were prepared by plating copper onto the fibres. The solutions and operating conditions for copper plating have been described elsewhere [3]. The volume fraction of fibre, V_f, in the composites was adjusted in steps of 0.07 by varying the thickness of the copper layer. All the specimens were annealed under vaccum at 1000 K for 7.2×10^3 sec to remove possible residual stresses induced during plating. The true strains at ultimate loadings were 0.22 and 0.37 for fibre and matrix respectively. The five parameters listed above were then measured at 0.12 and 0.20 true strains which are present in stage III-(1).

Tensile tests were conducted with an Instron-type tensile testing machine at 195 and 220 K in methanol and liquid baths. The flow stress was measured by simple tensile tests. Internal stress was measured by an incremental unloading test [6], and then the effective stress was calculated by subtracting internal stress from flow stress. Changes in flow stress due to change in strain-rate and temperature were measured by the strain-rate and temperature cycling tests. The stress exponent of strain-rate, effective stress exponent of dislocation velocity, activation volume and activation enthalpy were obtained in due course [11, 12]. Simple tensile tests were made at 195 K by straining specimens at a strain-rate of 4.2×10^{-4} sec^{-1}. In incremental unloading tests to measure the internal stress at 195 K, specimens were first strained at 4.2×10^{-4} sec^{-1} strain-rate up to 0.12 and 0.20 true strains, and the load was incrementally unloaded for 300 sec with a step of 2 N until the negative relaxation was observed. The strain-rate cycling tests at 195 K were performed by increasing the strain-rate by a factor of 10 and subsequently decreasing the strain-rate by the same factor, where the base strain-rate was 4.2×10^{-4} sec^{-1}. The temperature cycling tests were carried out between 195 and 220 K, where the base temperature was 195 K.

3. Results and discussion

3.1. Flow stress, internal stress and effective stress

The flow stress of composites, σ_c, at true strains $\epsilon = 0.12$ and 0.20 are shown as a function of volume fraction of fibre, V_f, in Fig. 1. The solid line presents the ROM relation [1, 2] given by

$$\sigma_c = \sigma_f V_f + \sigma_m V_m, \qquad (1)$$

where σ and V are flow stress and volume fraction, and the subscripts c, f and m refer to composite, fibre and matrix, respectively. The measured values are in good agreement with the ROM prediction, as is widely ascertained.

The internal stress $\sigma_{i,c}$ and effective stress σ_c^* of composites at the same strains are shown as a function of V_f in Fig. 1. It is clear that $\sigma_{i,c}$ and σ_c^* obey the ROM given by

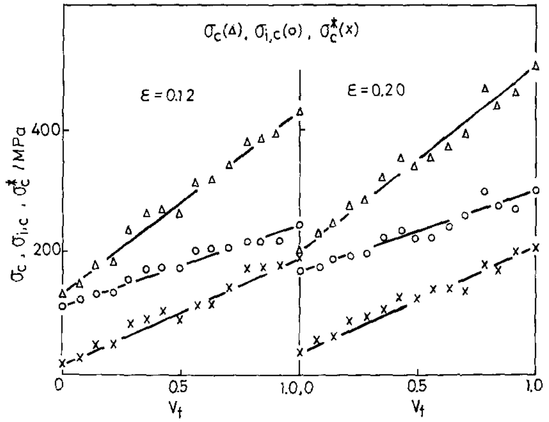

Figure 1 The measured values of $\sigma_c(\Delta)$, $\sigma_{i,c}(0)$ and $\sigma_c^*(\times)$ at $\epsilon = 0.12$ and 0.20 versus V_f.

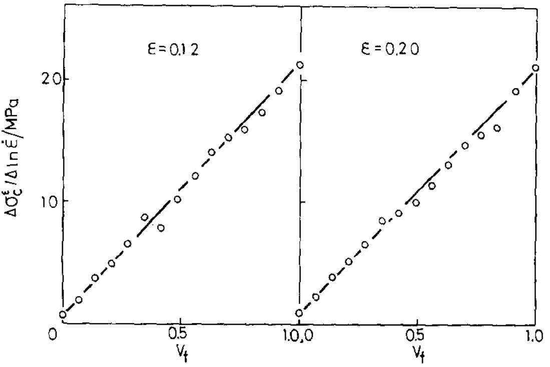

Figure 2 The measured values of $\Delta\sigma_c^{\dot\epsilon}/\Delta \ln \dot\epsilon$ at $\epsilon = 0.12$ and 0.20 versus V_f.

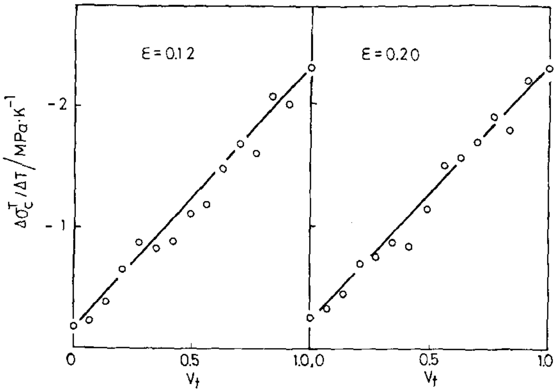

Figure 3 The measured values of $\Delta\sigma_c^T/\Delta T$ at $\epsilon = 0.12$ and 0.20 versus V_f.

$$\sigma_{i,c} = \sigma_{i,f} V_f + \sigma_{i,m} V_m \qquad (2)$$

$$\sigma_c^* = \sigma_f^* V_f + \sigma_m^* V_m. \qquad (3)$$

Equations 1 to 3 indicate that there is no interaction between the fibre and the matrix and that each component deforms as if it is deformed separately.

3.2. Change in flow stress due to change in strain-rate and to change in temperature

The change in flow stress of a composite due to change in strain-rate, $\Delta\sigma_c^{\dot{\epsilon}}$, and due to change in temperature, $\Delta\sigma_c^T$, are shown in Figs. 2 and 3 where $\Delta\sigma_c^{\dot{\epsilon}}/\Delta\ln\dot{\epsilon}$ and $\Delta\sigma_c^T/\Delta T$ are plotted as a function of V_f. It is obvious that both $\Delta\sigma_c^{\dot{\epsilon}}$ and $\Delta\sigma_c^T$ obey the ROM given by

$$\Delta\sigma_c^{\dot{\epsilon}} = \Delta\sigma_f^{\dot{\epsilon}} V_f + \Delta\sigma_m^{\dot{\epsilon}} V_m \tag{4}$$

$$\Delta\sigma_c^T = \Delta\sigma_f^T V_f + \Delta\sigma_m^T V_m. \tag{5}$$

It is widely noticed that the flow stress of a composite obeys the ROM, but to date it has not been investigated whether internal stress, effective stress and changes in flow stress due to change in strain-rate and temperature obey the ROM or not. This study first clarified that the above deformation parameters also obey ROM.

3.3. Stress exponent of strain-rate and effective stress exponent of dislocation velocity

The stress exponent of strain-rate, m, and effective stress exponent, m^*, are respectively given by

$$m = \partial\ln\dot{\epsilon}/\partial\ln\sigma \tag{6}$$

$$m^* = \partial\ln\dot{\epsilon}/\partial\ln\sigma^*. \tag{7}$$

Experimentally, we can obtain these parameters of composites (m_c and m_c^*) on the possible assumption that internal stress does not change at a given strain during the strain-rate cycling test, by employing the following equations:

$$m_c = \ln(\dot{\epsilon}_2/\dot{\epsilon}_1)/\ln((\sigma_c + \Delta\sigma_c^{\dot{\epsilon}})/\sigma_c) \tag{8}$$

$$m_c^* = \ln(\dot{\epsilon}_2/\dot{\epsilon}_1)/\ln((\sigma_c^* + \Delta\sigma_c^{\dot{\epsilon}})/\sigma_c^*), \tag{9}$$

where $\dot{\epsilon}_1$ and $\dot{\epsilon}_2$ are base and increased strain-rate and $\dot{\epsilon}_2/\dot{\epsilon}_1 = 10$ in this work.

Figs. 4 and 5 show the measured values of m_c and m_c^* at $\epsilon = 0.12$ and 0.20 as a function of V_f. In contrast with σ_c, $\sigma_{i,c}$, σ_c^*, $\Delta\sigma_c^{\dot{\epsilon}}$ and $\Delta\sigma_c^T$, m_c and m_c^* could not be determined by the volume-fraction weighted sum of m_f and m_m, and that of m_f^* and m_m^*, respectively. However, the interaction between the components is negligible as stated above, so that m_c and m_c^* must be determined only by the properties of each component. We can describe m_c only by using $V_f(V_m)$, σ_f, σ_m, m_f and m_m, and m_c^* by using $V_f(V_m)$, σ_f^*, σ_m^*, m_f^* and m_m^* as follows:

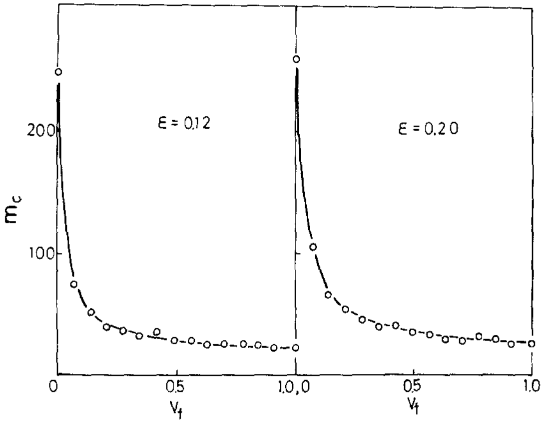

Figure 4 The measured values of m_c at $\epsilon = 0.12$ and 0.20 versus V_f.

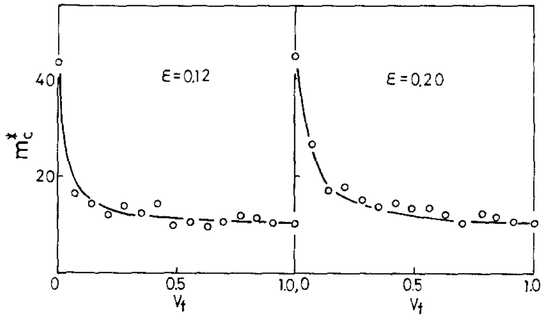

Figure 5 The measured values of m_c^* at $\epsilon = 0.12$ and 0.20 versus V_f.

Inserting $m_f = \partial\ln\dot{\epsilon}/\partial\ln\sigma_f$, $m_m = \partial\ln\dot{\epsilon}/\partial\ln\sigma_m$, and Equation 1 into $m_c = \partial\ln\dot{\epsilon}/\partial\ln\sigma_c$, we have

$$\frac{1}{m_c} = \frac{1}{m_f}\frac{\sigma_f V_f}{\sigma_f V_f + \sigma_m V_m} + \frac{1}{m_m}\frac{\sigma_m V_m}{\sigma_f V_f + \sigma_m V_m} \tag{10}$$

In a similar manner, we have

$$\frac{1}{m_c^*} = \frac{1}{m_f^*}\frac{\sigma_f^* V_f}{\sigma_f^* V_f + \sigma_m^* V_m} + \frac{1}{m_m^*}\frac{\sigma_m^* V_m}{\sigma_f^* V_f + \sigma_m^* V_m}. \tag{11}$$

Substituting the measured parameters of the fibre and the matrix at given strains, we have $m_c - V_f$ and $m_c^* - V_f$ relations shown with solid curves in Figs. 4 and 5, respectively. Equations 10 and 11 describe quite well the relations between m_c and V_f, and m_c^* and V_f, respectively.

Taking the case of m_c, we can represent m_c as

$$\frac{1}{m_c} = \frac{1}{m_f}\cdot\alpha + \frac{1}{m_m}\cdot(1-\alpha), \tag{12}$$

by putting $\sigma_f V_f/(\sigma_f V_f + \sigma_m V_m) = \alpha$. Equation 12 has the same form as the equation for obtaining the total resistivity of parallel resistances. We can interpret Equation 12 as the new form of the ROM, and Equations 10 and 11 as the modified ROMs for m_c and m_c^*, respectively.

3.4. Apparant activation volume

The activation volume, V^*, is given by

$$V^* = MkT \frac{\partial \ln \dot{\epsilon}}{\partial \sigma^{\dot{\epsilon}}}, \tag{13}$$

where M is the Taylor factor to combine the shear stress, τ, and tensile stress, σ; and shear strain, γ, and axial strain, ϵ, as

$$M = \sigma/\tau = \gamma/\epsilon; \tag{14}$$

k is Boltzmann's constant and T the absolute temperature. In the present paper, to obtain the apparent activation volume of composites, M was assumed to be 2.75 for 0.1% carbon-steel and 3.06 for copper, and for composites, it was inferred as follows.

As the fibre, matrix and composite are subjected to the same axial strain, γ_f, γ_m and γ_c are related to M_f, M_m and M_c as

$$\frac{\gamma_f}{M_f} = \frac{\gamma_m}{M_m} = \frac{\gamma_c}{M_c}. \tag{15}$$

Here we assume to a first approximation that the shear strain of the composite as a whole is given by the area (= volume) – fraction weighted sum of the shear strains of the fibre and matrix; namely

$$\gamma_c = \gamma_f V_f + \gamma_m V_m. \tag{16}$$

Combining Equations 15 and 16, we have

$$M_c = M_f V_f + M_m V_m. \tag{17}$$

(Of course, if we assume $M = 2$ for fibre, matrix and composite, as often assumed, the following treatment becomes simpler.)

Substituting the measured values of $\Delta \ln \dot{\epsilon}/\Delta\sigma_c^{\dot{\epsilon}}$ into $V_c^* = M_c kT \Delta \ln \dot{\epsilon}/\Delta\sigma_c^{\dot{\epsilon}}$, we have V_c^* as shown in Fig. 6.

As $\Delta\sigma_c^{\dot{\epsilon}}$ is given by Equation 4, V_c^* shall be given by

$$V_c^* = M_c kT \frac{\partial \ln \dot{\epsilon}}{\partial \sigma_c^{\dot{\epsilon}}} = M_c kT \frac{\partial \ln \dot{\epsilon}}{V_f \partial\sigma_f^{\dot{\epsilon}} + V_m \partial\sigma_m^{\dot{\epsilon}}}. \tag{18}$$

Inserting $V_f^* = M_f kT\ (\partial \ln \dot{\epsilon}/\partial\sigma_f^{\dot{\epsilon}})$, $V_m^* = M_m kT\ (\partial \ln \dot{\epsilon}/\partial\sigma_m^{\dot{\epsilon}})$ and Equation 17 into Equation 18, we have

$$\frac{1}{V_c^*} = \frac{1}{V_f^*} \cdot \frac{M_f V_f}{M_f V_f + M_m V_m} + \frac{1}{V_m^*} \cdot \frac{M_m V_m}{M_f V_f + M_m V_m}. \tag{19}$$

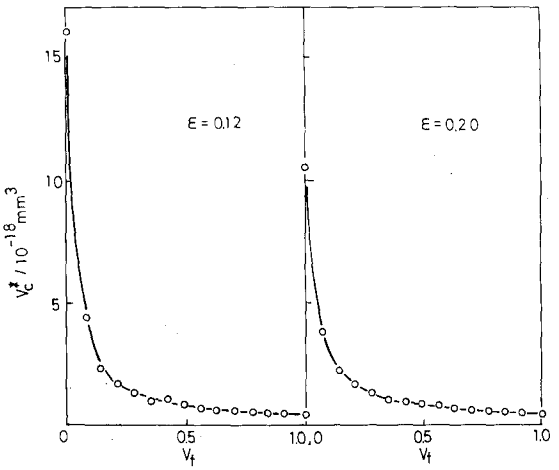

Figure 6 The measured values of V_c^* at $\epsilon = 0.12$ and 0.20 versus V_f.

Using the measured and known parameters of each component, we can calculate the $V_c^* - V_f$ relation. The result is shown as the solid curve in Fig. 6, indicating that Equation 19 is a good approximation for V_c^* in spite of the unverified assumption of Equation 16. In the present work, it was shown that V_c^* is determined only by the parameters of the fibre and the matrix. Equation 19 is regarded as the ROM for V_c^* since if we put $M_f V_f/(M_f V_f + M_m V_m) = \alpha$, Equation 19 becomes

$$\frac{1}{V_c^*} = \frac{1}{V_f^*} \cdot \alpha + \frac{1}{V_m^*} \cdot (1 - \alpha). \tag{20}$$

3.5. Activation enthalpy

The activation enthalpy, H, is given by

$$H = -kT^2 \left(\frac{\partial \ln \dot{\epsilon}}{\partial \sigma^{\dot{\epsilon}}}\right)_T \left(\frac{\partial \sigma^T}{\partial T}\right)_{\dot{\epsilon}} \tag{21}$$

Combining Equations 13 and 21, we have

$$H = -\frac{V^* T}{M} \left(\frac{\partial \sigma^T}{\partial T}\right)_{\dot{\epsilon}}. \tag{22}$$

Substituting the measured values of V_c^* shown in Fig. 6, T, M_c given by Equation 17 and $\Delta\sigma_c^T/\Delta T$ shown in Fig. 3 into Equation 22, we have the values of H_c as shown in Fig. 7.

TABLE I Summary of the ROMs for σ_c, $\sigma_{i,c}$, σ_c^*, $\Delta\sigma_c^{\dot\epsilon}$, $\Delta\sigma_c^T$, m_c, m_c^*, V_c^* and H_c

$\sigma_c = \sigma_f \cdot \alpha + \sigma_m \cdot (1-\alpha)$	$\alpha = V_f$	$\frac{1}{m_c} = \frac{\alpha}{m_f} + \frac{1-\alpha}{m_m}$	$\alpha = \frac{\sigma_f V_f}{\sigma_f V_f + \sigma_m V_m}$
$\sigma_{i,c} = \sigma_{i,f} \cdot \alpha + \sigma_{i,m} \cdot (1-\alpha)$	$\alpha = V_f$	$\frac{1}{m_c^*} = \frac{\alpha}{m_f^*} + \frac{1-\alpha}{m_m^*}$	$\alpha = \frac{\sigma_f^* V_f}{\sigma_f^* V_f + \sigma_m^* V_m}$
$\sigma_c^* = \sigma_f^* \cdot \alpha + \sigma_m^* \cdot (1-\alpha)$	$\alpha = V_f$	$\frac{1}{V_c^*} = \frac{\alpha}{V_f^*} + \frac{1-\alpha}{V_m^*}$	$\alpha = \frac{M_f V_f}{M_f V_f + M_m V_m}$
$\Delta\sigma_c^T = \Delta\sigma_f^T \cdot \alpha + \Delta\sigma_m^T \cdot (1-\alpha)$	$\alpha = V_f$	$H_c = H_f \cdot \alpha + H_m \cdot (1-\alpha)$	$\alpha = \frac{M_f V_f / V_f^*}{(M_f V_f / V_f^*) + (M_m V_m / V_m^*)}$

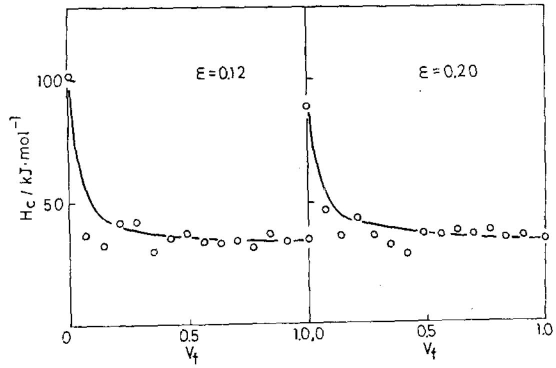

Figure 7 The measured values of H_c at $\epsilon = 0.12$ and 0.20 versus V_f.

Inserting Equations 5, 17 and 19 into

$$H_c = -\frac{V_c^* T}{M_c}\left(\frac{\partial\sigma_c^T}{\partial T}\right),$$

we have

$$H_c = \frac{H_f \cdot (M_f V_f/V_f^*) + H_m \cdot (M_m V_m/V_m^*)}{(M_f V_f/V_f^*) + (M_m V_m/V_m^*)}. \tag{23}$$

Substituting the parameters of H, M and V^* of the fibre and matrix, we have the $H_c - V_f$ relation as shown as the solid curve in Fig. 7. It is obvious that H_c can be predicted only by knowing the parameters of the components, and Equation 23 is, of course, regarded as the ROM since it becomes

$$H_c = H_f \cdot \alpha + H_m \cdot (1-\alpha) \tag{24}$$

if we put $(M_f V_f/V_f^*)/(M_f V_f/V_f^* + M_m V_m/V_m^*) = \alpha$.

Thus the parameters of composites in stage III-(1) investigated in this work may be described only by the properties of the components, indicating that the interaction between the components is, as expected, too small to be detected. Table I gives a summary of the ROM for each parameter.

4. Conclusions

Flow stress, internal stress, effective stress, change in flow stress due to change in strain-rate and temperature, stress exponent of strain-rate, effective stress exponent of dislocation velocity, activation volume and activation enthalpy of composites were measured in the deformation stage, where the mechanical interaction between the components is negligible, by using single carbon-steel fibre–copper matrix composites. It was found that all the parameters were determined only by the parameters of the components. For each parameter, the rule of mixtures was derived.

References

1. D. L. McDANELS, R. W. JECH and J. W. WEETON, *Trans. Met. Soc. AIME* **233** (1965) 636.
2. A. KELLY and W. R. TYSON, *J. Mech. Phys. Solids* **13** (1965) 329.
3. S. OCHIAI, K. SHIMOMURA and Y. MURAKAMI, *Met. Sci.* **9** (1975) 535.
4. R. HILL, *J. Mech. Phys. Solids* **12** (1964) 199, 213.
5. H. R. PIEHLER, *Trans. Met. Soc. AIME* **233** (1965) 12.
6. S. R. MACEWEN, O. A. KUPCIS and B. RAMASWAMI, *Scripta Met.* **3** (1969) 441.
7. I. GUPTA and J. C. LI, *Met. Trans.* **1** (1970) 2323.
8. G. GARMONG and L. A. SHEPARD, *ibid* **2** (1971) 175.
9. A. KELLY and H. LILHOLT, *Phil. Mag.* **20** (1969) 311.
10. K. NAKAZAWA and S. UMEKAWA, *J. Jap. Inst. Metals* **36** (1972) 398.
11. A. R. ROSENFIELD, G. T. HAHN, A. L. BEMENT, Jun. and R. T. JAFFEE, Eds., "Dislocation Dynamics", (McGraw-Hill, New York, 1968).
12. H. CONRAD, *J. Metals* **16** (1964) 582.

Received 20 July and accepted 18 September 1978.